

Re-analysis of the $^{24}\text{Mg}(\alpha, \gamma)^{28}\text{Si}$ reaction rate at stellar temperatures

P. Adsley,^{1,2,3,*} A. M. Laird,^{4,†} and Z. Meisel^{5,‡}

¹*School of Physics, University of the Witwatersrand, Johannesburg 2050, South Africa*

²*iThemba Laboratory for Accelerator Based Sciences, Somerset West 7129, South Africa*

³*Institut de Physique Nucléaire d'Orsay, UMR8608,*

IN2P3-CNRS, Université Paris Sud 11, 91406 Orsay, France

⁴*Department of Physics, University of York, Heslington, York, YO10 5DD, United Kingdom*

⁵*Institute of Nuclear and Particle Physics, Department of Physics & Astronomy, Ohio University, Athens, Ohio 45701, USA*

(Dated: December 30, 2019)

Background: The $^{24}\text{Mg}(\alpha, \gamma)^{28}\text{Si}$ reaction influences the production of magnesium and silicon isotopes during carbon burning and is one of eight reaction rates found to significantly impact the shape of calculated X-ray burst light curves. The reaction rate is based on measured resonance strengths and known properties of levels in ^{28}Si .

Purpose: It is necessary to update the astrophysical reaction rate for $^{24}\text{Mg}(\alpha, \gamma)^{28}\text{Si}$ incorporating recent modifications to the nuclear level data for ^{28}Si , and to determine if any additional as-yet unobserved resonances could contribute to the $^{24}\text{Mg}(\alpha, \gamma)^{28}\text{Si}$ reaction rate.

Methods: The reaction rate has been recalculated incorporating updated level assignments from $^{28}\text{Si}(\alpha, \alpha')^{28}\text{Si}$ data using the **RatesMC** Monte-Carlo code using updated nuclear data. Evidence from the $^{28}\text{Si}(p, p')^{28}\text{Si}$ reaction suggests that there are no further known resonances which could increase the reaction rate at astrophysically important temperatures, though some resonances do not yet have measured resonance strengths.

Results: The reaction rate is substantially unchanged from previously calculated rates, especially at astrophysically important temperatures. Increases in the reaction rate could occur at lower temperatures due to as-yet unmeasured resonances.

Conclusion: The $^{24}\text{Mg}(\alpha, \gamma)^{28}\text{Si}$ reaction rate, at temperatures relevant to carbon burning and Type I X-ray bursts, is well constrained by the available experimental data. This removes one reaction from the list of eight previously found to be important for X-ray burst light curve model-observation comparisons.

The $^{24}\text{Mg}(\alpha, \gamma)^{28}\text{Si}$ reaction plays a role in stellar environments, namely in X-ray bursts, during carbon burning in massive stars and in neon burning, at temperatures from 0.5 to 2 GK. In the case of Type I X-ray bursts, recent studies by Cyburt *et al.* [1] (using the CF88 rate of Caughlan and Fowler [2]) and Meisel *et al.* [3] (using the rate of Strandberg [4]) have shown that the burst composition in the A=24, 28-30 region and the resulting light-curve are both sensitive to the $^{24}\text{Mg}(\alpha, \gamma)^{28}\text{Si}$ reaction rate. This reaction is influential at temperatures between about 0.5 GK (Gamow window: $E_r = 700$ to 1220 keV [5]) and 1.0 GK (Gamow window: $E_r = 1010$ to 1710 keV [5]). In particular, an increase in the $^{24}\text{Mg}(\alpha, \gamma)^{28}\text{Si}$ reaction rate by a factor of ten from the default rate modifies the light-curve convexity, a measure of the shape of the rise of the light-curve, by 25% [3]. Decreasing the $^{24}\text{Mg}(\alpha, \gamma)^{28}\text{Si}$ reaction rate, however, had a much smaller impact [1].

The light-curve from X-ray bursts may, by comparison to models, be used to extract neutron-star properties such as mass and radius, as well as the accretion rate. However, the models and thus the neutron-star data extracted are sensitive to the thermonuclear reaction rates used. Once reaction rates are well constrained then their

potential influence on the light-curve may be minimised, reducing the uncertainty in the extraction of the neutron-star properties. Progress in constraining neutron star properties is particularly timely given the recent observation of a neutron star - neutron star merger (GW170817) and the detection of strontium in the resulting kilonova light curve [6].

In massive stars, ^{24}Mg is produced during carbon burning via the $^{20}\text{Ne}(\alpha, \gamma)^{24}\text{Mg}$ reaction following the conversion of two ^{12}C nuclei into ^{20}Ne by the reaction chains $^{12}\text{C}(^{12}\text{C}, \alpha)^{20}\text{Ne}$ and $^{12}\text{C}(^{12}\text{C}, p)^{23}\text{Na}(p, \alpha)^{20}\text{Ne}$. ^{24}Mg is subsequently destroyed by neutron- or α -particle capture making ^{25}Mg and ^{28}Si respectively. The abundances of magnesium and silicon isotopes depend on, amongst other factors, the relative strengths of the capture reactions onto ^{24}Mg within the relevant temperature range of 1 to 1.4 GK associated with carbon-shell burning [4].

The available nuclear data above the α -particle threshold at 9.984 MeV up to $E_x = 12$ MeV ($E_r = 2000$ keV) are summarised in a table found in the Supplementary Material. The sources of resonance strengths are the direct measurements performed by Smulders and Endt [7], Lyons [8] and Strandberg *et al.* [4]. Spectroscopic information is available from the γ -ray spectroscopy data obtained in $^{27}\text{Al}(p, \gamma)^{28}\text{Si}$ and $^{24}\text{Mg}(\alpha, \gamma)^{28}\text{Si}$ reactions of Brennesien *et al.* [9–11], the $^{28}\text{Si}(\alpha, \alpha')^{28}\text{Si}$ data of Adsley *et al.* [12], and the $^{28}\text{Si}(p, p')^{28}\text{Si}$ data of Adsley *et al.* [13]. We briefly summarise these experimental data and the information obtained from them below.

Maas *et al.* [14], and Smulders and Endt [7] studied

* philip.adsley@wits.ac.za

† alison.laird@york.ac.uk

‡ meisel@ohio.edu; Affiliated with the Joint Institute for Nuclear Astrophysics Center for the Evolution of the Elements

the $^{24}\text{Mg}(\alpha, \gamma)^{28}\text{Si}$ reaction using a 10 cm x 10 cm NaI crystal, measuring strengths for resonances from $E_r = 3246$ ($E_\alpha = 3787$ keV) down to $E_r = 1311$ keV ($E_\alpha = 1530$ keV). Smulders and Endt additionally performed angular-correlation analyses on resonances observed in $^{24}\text{Mg}(\alpha, \gamma)^{28}\text{Si}$ and $^{27}\text{Al}(p, \gamma)^{28}\text{Si}$ reactions in order to assign spins and parities. Both of these experimental studies measured yield curves with energy scans rather than only performing on-resonance measurements.

Lyons [8] measured yield curves from a maximum resonance energy of $E_r = 2317$ keV ($E_\alpha = 2703$ keV) down to the resonance at $E_r = 1164$ keV ($E_\alpha = 1358$ keV). Two NaI crystals in close geometry, functioning as a total-absorption spectrometer were used to measure the yields from the $^{24}\text{Mg}(\alpha, \gamma)^{28}\text{Si}$ reaction. The same experimental equipment had already been used to measure the $^{27}\text{Al}(p, \gamma)^{28}\text{Si}$ reaction [15]. In this experiment, resonances were observed down to $E_r = 1158$ keV. Lyons also performed yield curves by scanning the energy of the incoming beam.

The experimental data of Strandberg *et al.* [4] scanned energies between $E_r = 1337$ keV ($E_\alpha = 1560$ keV) and $E_r = 909$ keV ($E_\alpha = 1060$ keV). More detailed data were taken at specific resonance energies focusing on known or potential natural parity states, chosen based on the existing data on excited states in ^{28}Si . Data were taken in smaller energy steps to scan over the resonances in question. Four NaI(Tl) and one HPGe clover were used to detect γ rays resulting from $^{24}\text{Mg}(\alpha, \gamma)^{28}\text{Si}$ reactions. The detectors were operated in coincidence mode with the NaI(Tl) crystals detecting the high-energy primary γ ray, with the clover detecting the $E_\gamma = 1779$ -keV transition from the first-excited state to the ground state. The $E_r = 1311$ -keV resonance which had been observed by Smulders and Endt, Maas, and Lyons was remeasured, allowing potential systematic deviations between data to be identified. Resonance strengths were measured for resonances down to $E_r = 1010$ keV. Below this energy (corresponding to $E_\alpha = 1178$ keV) no resonances were observed but upper limits on the resonance strengths for all lower lying resonances were determined.

Brenneisen *et al.* [9–11] measured the $^{24}\text{Mg}(\alpha, \gamma)^{28}\text{Si}$ ($E_\alpha = 1.5 - 4$ MeV) and $^{27}\text{Al}(p, \gamma)^{28}\text{Si}$ ($E_p = 0.63 - 4.85$ MeV) reactions to assign spins and parities of levels in ^{28}Si . Information on resonance strengths in the astrophysically important region were not given.

The $^{28}\text{Si}(\alpha, \alpha')^{28}\text{Si}$ reaction has been measured at iThemba LABS in South Africa using the K600 at very forward angles including 0 degrees [12]. From the differential cross section the ℓ -value, and therefore spin and parity, for the state could be derived. Following this experiment two changes to the spin and parity assignments of ^{28}Si levels were made. First, the $E_x = 10.806$ -MeV level assignment was changed from $J^\pi = 2^+$ to $J^\pi = 0^+$ and, second, a $J^\pi = 0^+$ level at $E_x = 11.142$ MeV was observed in addition to a known $J^\pi = 2^+$ level at $E_x = 11.148$ MeV.

Data on the $^{28}\text{Si}(p, p')^{28}\text{Si}$ reaction with the Q3D spec-

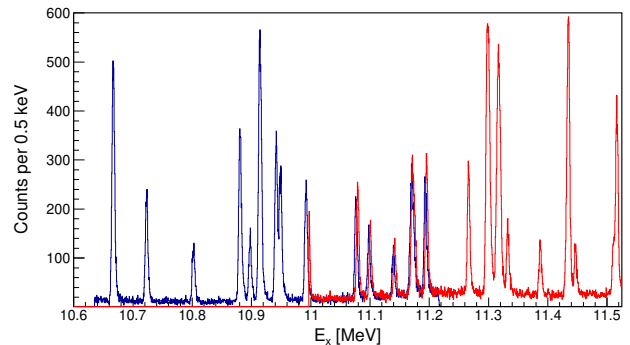


FIG. 1. Excitation-energy spectrum from the $^{28}\text{Si}(p, p')^{28}\text{Si}$ reaction at field settings 1 (blue) and 2 (red).

trometer at the Maier-Leibnitz-Laboratorium (MLL), Garching, Germany, were taken using a 18-MeV proton beam on a $40\text{-}\mu\text{g}/\text{cm}^2$ -thick $^{28}\text{SiO}_2$ target on a carbon backing. These data were published as a calibration spectrum and as evidence of the selectivity of the $^{28}\text{Si}(d, d')^{28}\text{Si}$ reaction to $\Delta T = 0$ transitions as part of an experiment investigating levels in ^{26}Mg [13].

An excitation-energy spectrum from the $^{28}\text{Si}(p, p')^{28}\text{Si}$ reaction is shown in Fig. 1. Data were taken in two different exposures at different field settings with an overlapping region in the centre. Almost all peaks correspond to states in ^{28}Si : the two levels at approximately $E_x = 11.3$ MeV are the $E_x = 11.080$ - and $E_x = 11.097$ -MeV state in ^{16}O , and the $E_x = 10.957$ -MeV state in ^{16}O is observed at around $E_x = 11.17$ MeV. An $E_x = 11.242$ -MeV state which was assigned from a $^{27}\text{Al}(d, n)^{28}\text{Si}$ reaction [16] is not observed and we suggest that this state should be omitted from future compilations.

All of the levels observed in the $^{28}\text{Si}(p, p')^{28}\text{Si}$ reaction of Ref. [13] correspond to known levels in ^{28}Si . The experimental resolution is around 5 keV FWHM and there may be additional states which are unresolved. However, as can be seen in Fig. 1, the observed peaks are generally isolated and well-separated and so it is unlikely that a large number of additional states are present but unresolved and therefore unobserved.

In order to estimate the reaction rate with robust uncertainties, we used a publicly available Monte-Carlo code, RatesMC [17]. RatesMC is a code available as part of the STARLIB project [18] which calculates reaction rates using a Monte-Carlo technique. This approach allows for the evaluation of the reaction rate with meaningful uncertainties based on the uncertainties in the experimental data. For details as to how RatesMC operates refer to Refs. [19, 20]. We briefly summarise here the assumptions made in preparing the inputs for RatesMC, taking into account the remaining uncertainties in the nuclear data.

For narrow resonances the reaction rate at a given temperature is determined from the resonance strengths and energies using [21]:

$$N_A \langle \sigma v \rangle = \frac{1.5399 \times 10^{11}}{(\mu T_9)^{\frac{3}{2}}} \sum_i (\omega \gamma)_i e^{-11.605 E_{r,i}/T_9}, \quad (1)$$

given in $\text{cm}^3 \text{mol}^{-1} \text{s}^{-1}$, where the sum is over the narrow resonances, $E_{r,i}$ is the resonance energy of the i th resonance, $(\omega \gamma)_i$ is the resonance strength of the i th resonance, μ is the reduced mass, and T_9 is the temperature in GK. For all of the resonances considered in this paper the α -particle partial width is much smaller than the γ -ray partial width meaning that $\omega \gamma \approx (2J + 1)\Gamma_\alpha$ where J is the spin of the resonance and Γ_α is the α -particle partial width; the resonance strength is determined by the α -particle partial width. Resonance strengths determined from thick-target measurements are insensitive to the spin and parity of the underlying resonance; changes to spin-parity assignments will leave the astrophysical reaction rate unchanged.

For cases where the spin and parity of a resonance are known but resonance strength or the partial widths are not, it is possible to estimate the possible contribution of the resonance to the reaction rate. The upper limit on the partial width may be calculated using the Wigner limit [22] or some other single-particle width based on realistic wave-functions and these upper limits used to estimate the reaction rate. Various different approaches are available including calculating the rate assuming a mean value for the reduced width [4], calculating an upper limit based on upper limits for the reduced widths for cluster states [23], or, as in the present case, using a Monte-Carlo method where the reduced width is drawn from a probability distribution function [17].

In the present evaluation upper limits for resonance strengths have been calculated for all resonances below the lowest measured resonance ($E_r = 1010$ keV) in the experimental study of Strandberg *et al.* [4]. For calculation of the reaction rates the limit for the resonance strength is the lower of the limit from the Strandberg data ($\sum \omega \gamma < 2 \times 10^{-6}$ eV) for all resonances at $E_r \leq 909$ keV and the resonance strength assuming the Wigner limit for the α -particle partial width. For the estimation of the contribution from the upper limits of resonances the `RatesMC` code generates Γ_α partial widths assuming that the reduced widths follow a Porter-Thomas distribution with $\langle \theta^2 \rangle = 0.01$ following systematic trends, for more details see Refs. [24]. We assume the same distribution for levels which have experimental upper limits, but use the experimental upper limit instead of the Wigner limit.

To account for the changes to the ^{28}Si level structure from Ref. [12], the reaction rate was recalculated with various different assumptions about the origin of the $^{24}\text{Mg}(\alpha, \gamma)^{28}\text{Si}$ cross section around $E_x = 11.14 - 11.15$ MeV, these different assumptions were found to have a negligible impact on the total reaction rate. We assumed that 90% of the strength originates from the $E_x = 11.142$ -MeV state which has $J^\pi = 0^+$ and 10% from the $E_x = 11.148$ -MeV state which has $J^\pi = 2^+$.

The STARLIB evaluation of the $^{24}\text{Mg}(\alpha, \gamma)^{28}\text{Si}$ reaction rate did not include some low-lying resonances. We have evaluated the reaction rate including only those resonances in the STARLIB evaluation (denoted ‘Subset’ in Fig. 2) and, additionally, including all isoscalar natural-parity resonances but omitting the $J^\pi = 3^-$ state at $E_x = 11.266$ MeV and any states known to be isovector in nature. This second reaction rate is denoted ‘All’ in Fig. 2. The reaction rate evaluated with an increased set of resonances quantifies the potential increase in the reaction rate due to low-energy resonances. The state at $E_x = 11.266$ MeV is omitted as that resonance energy has been scanned in direct measurements in multiple experiments and no resonance has been observed. It is not possible to provide an experimental upper limit based on the available knowledge of those experimental studies. Tab. I in the Supplementary Material gives the nuclear data inputs for the resonances used for the calculation of the reaction rates.

To account for unknown systematic effects in the resonance strengths we considered the variation in the measured values of the $E_r = 1311$ -keV resonance which was measured in the Strandberg, Lyons, Maas, and Smulders and Endt experiments. The resonance strengths determined in these experiments agree extremely well (χ^2 per degree-of-freedom of 0.28) assuming a 30% error in the absolute measurement of Smulders and Endt. We do not adopt the procedure described in Ref. [24] to account for additional systematic variations.

The ratio of various reaction rates to the STARLIB reference rate are shown in Fig. 2. The reaction rates displayed include those calculated in the present study under various different assumptions for the nuclear data, the reaction rate from Caughlan and Fowler (CF88) [2], and Strandberg *et al.* [4]. A reaction rate calculated using TALYS (version 1.8) [25] with the α particle-nucleus optical-model potential calculated by Watanabe folding of the Koning-Delaroche nucleon potentials is also displayed, as is the reaction rate from the NON-SMOKER compilation [26].

The reaction rate calculated in the present paper using the STARLIB subset of states is consistent with the STARLIB evaluation. Above 0.4 GK, no significant variations in the reaction rate are observed depending on the choice of the nuclear data. Changes to the assumptions of the observed strength between $E_x = 11.14$ and 11.15 MeV, or the spin-parity assignment of the level at $E_x = 10.806$ MeV have little effect on the final reaction rate.

The addition of the low-lying resonances omitted in the STARLIB evaluation causes a modest increase in the reaction rate below 0.4 GK. The increase is comfortably below the temperatures of the astrophysical scenarios in which the $^{24}\text{Mg}(\alpha, \gamma)^{28}\text{Si}$ reaction plays a role.

The rates calculated in the present work are significantly higher at low temperatures than the Strandberg *et al.* [4] rate. This is likely due to the different treatments of the α -particle partial widths in the current Monte-

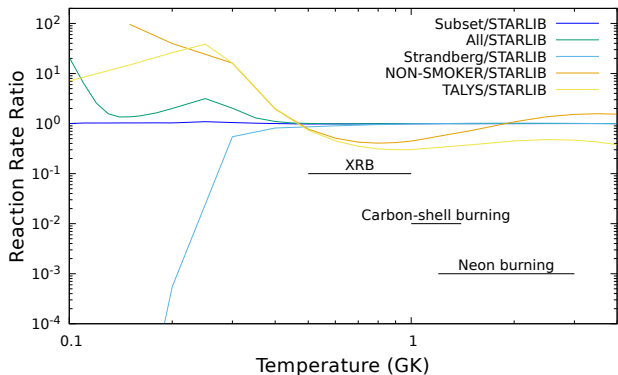


FIG. 2. Reaction-rate ratios relative to the STARLIB reaction rate for the reaction rates calculated in the present paper, the rate of Strandberg *et al.* [4], and reaction rates taken from the statistical-model codes TALYS [25] and NON-SMOKER [26].

Carlo calculations. However such low temperatures are not relevant to the astrophysical sites considered here.

The reaction rates from TALYS and NON-SMOKER over-predict the rate until around 0.4 GK, at which point both begin to under-predict the reaction rate. This is potentially due to the statistical models over-predicting other reaction channels such as $^{24}\text{Mg}(\alpha, p)^{27}\text{Al}$ or under-predicting the strength of decay γ -ray transitions.

The fractional contributions of individual resonances to the total reaction rate are shown in Fig. 3. From Fig. 3, additional resonances would have to lie above $E_r = 1010$ keV ($E_x = 10.994$ MeV) to cause increases to the reaction rate in the astrophysically important temperature region. Strong resonances above $E_r = 1010$ keV would have been observed in the numerous $^{24}\text{Mg}(\alpha, \gamma)^{28}\text{Si}$ direct measurements [4, 7, 8, 14]. Large increases in the $^{24}\text{Mg}(\alpha, \gamma)^{28}\text{Si}$ reaction rate at astrophysically important temperatures due to unobserved resonances above $E_r = 1010$ keV can therefore be ruled out.

The relative uncertainty in the $^{24}\text{Mg}(\alpha, \gamma)^{28}\text{Si}$ relative to the median reaction rate is shown in Fig. 4. Above 0.4 GK the reaction rate is well constrained on the basis of the measured resonance strengths. Below 0.4 GK the reaction rate is dominated by unmeasured resonances which do not have known or estimated resonance strengths, in particular the $E_r = 197$ -, 327 -, 530 -, 557 - and 684 -keV resonances (see Fig. 3). The α -particle partial widths are the dominant sources of uncertainty for the reaction rate below 0.4 GK.

Tables of the $^{24}\text{Mg}(\alpha, \gamma)^{28}\text{Si}$ median and 68% confidence limit upper and lower limits reaction rates calculated using the STARLIB subset and the complete set of possible resonances are given in the Supplementary Material, along with REACLIB parameterisations of the reaction rate between 0.1 and 2.5 GK according to the prescription in Ref. [27].

The re-analysed $^{24}\text{Mg}(\alpha, \gamma)^{28}\text{Si}$ reaction rate was used in the model of Refs. [3, 28] to determine if the re-

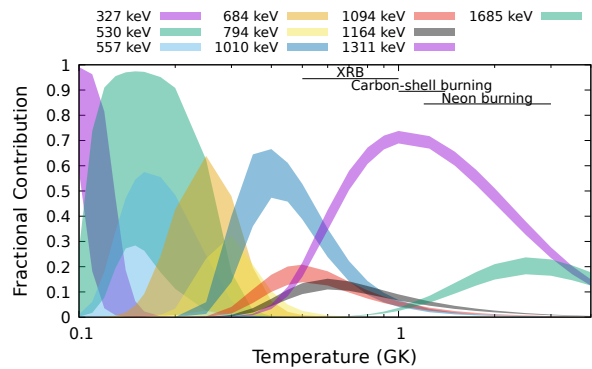


FIG. 3. Fractional contribution plot of individual resonances to the $^{24}\text{Mg}(\alpha, \gamma)^{28}\text{Si}$ reaction rate, calculated using the complete set of possible additional resonances. Only resonances which contribute significantly to the reaction rate are plotted; the sum of the plotted contributions is below 100% at some temperatures. The temperature regions corresponding to X-ray burst, carbon-shell burning and neon burning are also shown. The impact of potential new resonances ($E_r \leq 794$ keV) on the reaction rate is limited to temperatures below the astrophysically important temperature ranges.

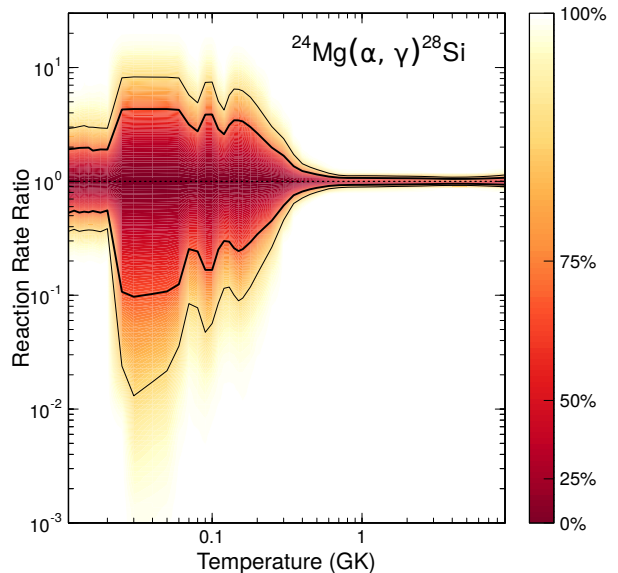


FIG. 4. Reaction-rate uncertainty bands for scenario IV. The colour represents the probability distribution function while the 68% and 95% confidence limits are denoted by thick and thin black lines respectively.

maining uncertainty in the reaction rate causes any discernible variation in the behaviour of the X-ray burst lightcurve. One-dimensional model calculations were performed with the code MESA [29–31] version 9793, following the thermodynamic and nucleosynthetic evolution of an ~ 0.01 km thick envelope of material discretized into ~ 1000 zones with an inner boundary of an 11.2 km $1.4 M_{\odot}$ neutron star. Notable microphysics included

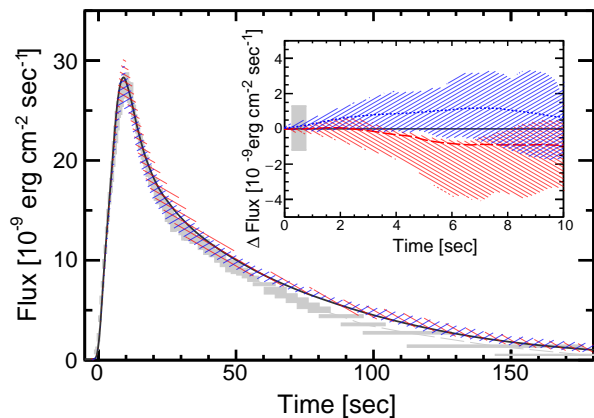


FIG. 5. X-ray burst light curve 68% confidence interval bands calculated with MESA using the median (black line), upper 95% (red-hash area), and lower 95% (blue-hash area) STARLIB reaction rates for $^{24}\text{Mg}(\alpha, \gamma)^{28}\text{Si}$, compared to observations of the year 2007 bursting epoch of GS 1826-24 (gray boxes) for context. The inset shows the residual over the light curve rise to MESA results obtained with the median STARLIB rate, where the gray box indicates the average observational uncertainty in that time frame. Note that the MESA light curve bands are asymmetric uncertainties, where the dashed or dotted line indicates the average, with the uncertainty for a single band owing to burst-to-burst variability.

time-dependent mixing-length theory for convection [32], a post-Newtonian correction to local gravity for general relativistic effects [29], and the 304 isotope network of Ref. [33] employing the REACLIBv2.2 nuclear reaction rate library [27]. The accretion conditions used were those found by Ref. [28] to best reproduce the observed features of the year 2007 bursting epoch of the source GS 1826-24 [34].

Average light curves were calculated from a sequence of 14 X-ray bursts, employing either the median, upper 95% confidence limit, or lower 95% confidence limit for the $^{24}\text{Mg}(\alpha, \gamma)^{28}\text{Si}$ reaction rate calculated using RatesMC. Results are shown in Fig. 5 alongside observational data [34] for GS 1826-24 for context. The figure inset shows the residual between calculation results using the median rate and upper and lower 95% confidence intervals for the rising portion of the X-ray burst light curve. Whereas the previously assumed factor of 10 uncertainty resulted in an appreciably different convexity of the light curve rise [3], the present rate uncertainty causes light curve variations on the order of observational uncertainties and the intrinsic burst-to-burst variability of model calculations. Therefore, we find the $^{24}\text{Mg}(\alpha, \gamma)^{28}\text{Si}$ reaction rate uncertainty no longer ap-

preciably contributes to the overall uncertainty in the calculated X-ray burst light curve.

In summary, the available nuclear data on ^{28}Si relevant to the $^{24}\text{Mg}(\alpha, \gamma)^{28}\text{Si}$ reaction have been reviewed and the reaction rate recalculated on the basis of new level assignments. At astrophysically important temperatures the reaction rate is dominated by the $E_r = 1010, 1094, 1164,$ and 1311 keV resonances, with the last of these dominating the rate in the astrophysically relevant temperature range. Direct measurements of $^{24}\text{Mg}(\alpha, \gamma)^{28}\text{Si}$ resonance strengths are consistent and the level of uncertainty in the calculated reaction rate is small. The direct measurement data of Refs. [4, 7, 8, 14] include excitation functions over a range of incident energies, and therefore any unobserved resonances cannot be sufficiently strong to significantly increase the $^{24}\text{Mg}(\alpha, \gamma)^{28}\text{Si}$ reaction rate. Additional contributions from new states have been ruled out using $^{28}\text{Si}(p, p')^{28}\text{Si}$ data. This unselective reaction revealed no new states between the α -particle threshold and the lowest directly measured resonance.

The remaining uncertainty in the $^{24}\text{Mg}(\alpha, \gamma)^{28}\text{Si}$ reaction rate does not significantly alter the calculated X-ray burst light curve. Therefore, this reaction rate, one of eight identified as important for X-ray burst model-observation comparisons [3], is adequately constrained for the purposes of determining properties of accreting neutron star systems from such comparisons.

ACKNOWLEDGEMENTS

This paper is based upon work from the ‘ChETEC’ COST Action (CA16117), supported by COST (European Cooperation in Science and Technology). PA acknowledges and thanks the Claude Leon Foundation for a postdoctoral research fellowship and the NRF/iThemba LABS for support, and those who assisted in the collection of the $^{28}\text{Si}(\alpha, \alpha')^{28}\text{Si}$ data using the K600 magnetic spectrometer at iThemba LABS and $^{28}\text{Si}(p, p')^{28}\text{Si}$ data using the Q3D magnetic spectrograph at the Maier-Leibnitz Laboratorium in Munich. AML acknowledges the support of the U.K. Science and Technology Facilities Council (STFC Consolidated Grant ST/P003885/1). ZM acknowledges support from the U.S. Department of Energy Office of Science through Grants No. DE-FG02-88ER40387 and DESC0019042 and the U.S. National Science Foundation through Grant PHY-1430152 (Joint Institute for Nuclear Astrophysics – Center for the Evolution of the Elements). The authors thank Richard Longland for access to the RatesMC code and associated R scripts.

[1] R. H. Cyburt, A. M. Amthor, A. Heger, E. Johnson, L. Keek, Z. Meisel, H. Schatz, and K. Smith, The Astrophysical Journal **830**, 55 (2016).

[2] G. R. Caughlan and W. A. Fowler, Atomic Data and Nuclear Data Tables **40**, 283 (1988).

- [3] Z. Meisel, G. Merz, and S. Medvid, *The Astrophysical Journal* **872**, 84 (2019).
- [4] E. Strandberg, M. Beard, M. Couder, A. Couture, S. Falahat, J. Görres, P. J. LeBlanc, H. Y. Lee, S. O'Brien, A. Palumbo, E. Stech, W. P. Tan, C. Ugalde, M. Wiescher, H. Costantini, K. Scheller, M. Pignatari, R. Azuma, and L. Buchmann, *Phys. Rev. C* **77**, 055801 (2008).
- [5] T. Rauscher, *Phys. Rev. C* **81**, 045807 (2010).
- [6] D. Watson, C. J. Hansen, J. Selsing, A. Koch, D. B. Malesani, A. C. Andersen, J. P. Fynbo, A. Arcones, A. Bauswein, S. Covino, *et al.*, *Nature* **574**, 497 (2019).
- [7] P. Smulders and P. Endt, *Physica* **28**, 1093 (1962).
- [8] P. Lyons, *Nuclear Physics A* **130**, 25 (1969).
- [9] J. Brenneisen, D. Grathwohl, M. Lickert, R. Ott, H. Röpke, J. Schmalzlin, P. Siedle, and B. Wildenthal, *Zeitschrift für Physik A Hadrons and Nuclei* **352**, 149 (1995).
- [10] J. Brenneisen, D. Grathwohl, M. Lickert, R. Ott, H. Röpke, J. Schmalzlin, P. Siedle, and B. Wildenthal, *Zeitschrift für Physik A Hadrons and Nuclei* **352**, 279 (1995).
- [11] J. Brenneisen, D. Grathwohl, M. Lickert, R. Ott, H. Röpke, J. Schmalzlin, P. Siedle, and B. H. Wildenthal, *Zeitschrift für Physik A Hadrons and Nuclei* **352**, 403 (1995).
- [12] P. Adsley, D. G. Jenkins, J. Cseh, S. S. Dimitriova, J. W. Brümmer, K. C. W. Li, D. J. Marín-Lámbarri, K. Lukyanov, N. Y. Kheswa, R. Neveling, P. Papka, L. Pellegrini, V. Pseudo, L. C. Pool, G. Riczu, F. D. Smit, J. J. van Zyl, and E. Zemlyanaya, *Phys. Rev. C* **95**, 024319 (2017).
- [13] P. Adsley, J. W. Brümmer, T. Faestermann, S. P. Fox, F. Hammache, R. Hertzenberger, A. Meyer, R. Neveling, D. Seiler, N. de Séréville, and H.-F. Wirth, *Phys. Rev. C* **97**, 045807 (2018).
- [14] J. Maas, E. Somorjai, H. Graber, C. V. D. Wijngaart, C. V. D. Leun, and P. Endt, *Nuclear Physics A* **301**, 213 (1978).
- [15] P. Lyons, J. Toevs, and D. Sargood, *Nuclear Physics A* **130**, 1 (1969).
- [16] H. Satyanarayana, M. Ahmad, C. E. Brient, P. M. Egun, S. L. Graham, S. M. Grimes, and S. K. Saraf, *Phys. Rev. C* **32**, 394 (1985).
- [17] A. L. Sallaska, C. Iliadis, A. E. Champagne, S. Goriely, S. Starrfield, and F. X. Timmes, *The Astrophysical Journal Supplement Series* **207**, 18 (2013).
- [18] “Starlib,” <http://starlib.physics.unc.edu/> (2019), accessed: 6 January 2019.
- [19] A. L. Sallaska, C. Iliadis, A. E. Champagne, S. Goriely, S. Starrfield, and F. X. Timmes, *The Astrophysical Journal Supplement Series* **207**, 18 (2013).
- [20] C. Iliadis, R. Longland, A. Champagne, A. Coc, and R. Fitzgerald, *Nuclear Physics A* **841**, 31 (2010), the 2010 Evaluation of Monte Carlo based Thermonuclear Reaction Rates.
- [21] C. Iliadis, *Nuclear Physics of Stars*, Physics textbook (Wiley, 2008).
- [22] E. P. Wigner, *Phys. Rev.* **98**, 145 (1955).
- [23] G. Lotay, D. Doherty, D. Seweryniak, S. Almaraz-Calderon, M. Carpenter, C. Chiara, H. David, C. Hoffman, R. Janssens, A. Kankainen, *et al.*, *The European Physical Journal A* **55**, 109 (2019).
- [24] R. Longland, C. Iliadis, and A. I. Karakas, *Phys. Rev. C* **85**, 065809 (2012).
- [25] “Talys,” https://tendl.web.psi.ch/tendl_2019/talys.html, version 1.8.
- [26] T. RAUSCHER and F.-K. THIELEMANN, *Atomic Data and Nuclear Data Tables* **79**, 47 (2001).
- [27] R. H. Cyburt, A. M. Amthor, R. Ferguson, Z. Meisel, K. Smith, S. Warren, A. Heger, R. D. Hoffman, T. Rauscher, A. Sakharuk, H. Schatz, F. K. Thielemann, and M. Wiescher, *The Astrophysical Journal Supplement Series* **189**, 240 (2010).
- [28] Z. Meisel, *Astrophys. J.* **860**, 147 (2018).
- [29] B. Paxton, L. Bildsten, A. Dotter, F. Herwig, P. Lesaffre, and F. Timmes, *Astrophys. J. Suppl. Ser.* **192**, 3 (2011), www.mesa.sourceforge.net.
- [30] B. Paxton, M. Cantiello, P. Arras, L. Bildsten, E. F. Brown, A. Dotter, C. Mankovich, M. H. Montgomery, D. Stello, and F. X. Timmes, *Astrophys. J. Suppl. Ser.* **208**, 4 (2013).
- [31] B. Paxton, P. Marchant, J. Schwab, E. B. Bauer, L. Bildsten, M. Cantiello, L. Dessart, R. Farmer, H. Hu, and N. Langer, *Astrophys. J. Suppl. Ser.* **220**, 15 (2015).
- [32] L. Henry and J. L’Ecuyer, *The Astrophysical Journal* **156**, 549 (1969).
- [33] J. L. Fisker, H. Schatz, and F.-K. Thielemann, *Astrophys. J. Suppl. Ser.* **174**, 261 (2008).
- [34] D. K. Galloway, A. J. Goodwin, and L. Keek, *Publications of the Astronomical Society of Australia* **34** (2017), 10.1017/pasa.2017.12.